

A Novel Analytical Expressions Model for Corona Currents Based on Curve Fitting Method Using Artificial Neural Network

Gao Hui Fan*, Shang He Liu, Ming Wei, and Xiao Feng Hu

Abstract—The analytical expressions for corona discharge currents are usually represented by the mathematic models based on curve fitting method. For the complex mechanisms, none of these currently models can describe a measured corona current with arbitrary waveforms. A novel curve fitting method using BP neural network (BPNN) technique is applied to describe the mathematic model of the corona currents in time domain. The analytical expressions for the currents can be established via extracting the weights and thresholds parameters of the trained BPNN. The expressions all have the same structure which has only four types of parameters, and the structure is independent of the corona current waveforms. The curve fitting for the measured corona currents with arbitrary waveforms by different models was carried out, and the results were analyzed, which indicate that the BPNN method performs best. Compared with the current expressions fitted by the double exponential function and Gaussian function, the expressions by BPNN can fit the current waveforms with the lowest mean square error (MSE) in time domain and the highest accuracy to spectra of the currents in frequency domain. The proposed method is suitable for establishing a unified analytical expressions model for corona currents with arbitrary shapes.

1. INTRODUCTION

Corona discharge widely exists in high voltage transmission lines due to sufficiently high electric fields of line conductor surface. For a long time, these discharges often bring in eventual failure within insulators and electrical plant items such as power transformers and gas insulated switchgear [1]. In order to indicate and monitor these incipient discharges within the electrical system on-line, a number of measurement techniques have been developed, including acoustic, chemical, optical and electrical techniques. As a conventional electrical technique, the current measuring technique has great significance in on-line monitoring of the electrical plant items and analyzing of their performances. Direct measurement of corona discharge currents provides valuable data which can be used to define the excitation function more accurately for analytical studies and numerical modeling of corona discharge and associated phenomena [2–4]. However, a unified analytical expressions model for the corona currents has not been established. For the complex mechanism of corona discharge, it is difficult to illustrate the currents by analytical method. As a particular way to conveniently describe the measured currents, the curve fitting method is widely used. The developed curve fitting models to approximate to the current waveforms include the Wanninger function [5], double exponential function [6, 7] and Gaussian function [8]. These models are frequently utilized to investigate the discharge mechanisms and the radiated electromagnetic fields [9–12]. However, the corona current waveforms not only depend on their discharge mechanism characters, but also rely on the configurations of the measurement system, signal transmission paths and even the interference from ambient environment [13]. Therefore, corona currents

Received 16 November 2014, Accepted 22 January 2015, Scheduled 5 February 2015

* Corresponding author: Gaohui Fan (fangaohuioec@163.com).

The authors are with the Institute of Electrostatic and Electromagnetic Protection, Mechanical Engineering College, Shijiazhuang, China.

may display great difference among discharges. The three functions cited above are able to represent specific shapes, but none is more flexible and can match corona currents with arbitrary shapes well and easily. So it is necessary to establish a new and suitable analytical expressions model for corona currents with arbitrary shapes.

In order to extract the analytical expression for one arbitrary corona current, a novel method based on curve fitting using BPNN was proposed, and description of the mathematic model was developed in this paper. The BPNN will be trained by the data which includes the time sequence t and measured current magnitude $i(t)$. The training process is just the approach to the curve fitting of the current waveform. The analytical expression for the current can be derived by extracting the weights and thresholds parameters of the trained BPNN.

2. ANALYTICAL EXPRESSION MODELS FOR CORONA CURRENT BY CURVE FITTING METHOD

2.1. Currently Used Models

Currently the analytical expression models of partial discharge (PD), including corona discharge, are usually represented by the Wangnigner's function, double exponential function and Gaussian function. The current represented by the Wanninger's function is presented as:

$$I(t) = \frac{I_1}{T_1} t e^{1-t/T_1} \quad (1)$$

where I_1 is the peak amplitude, and T_1 governs the rise time.

The current represented by the double exponential function is shown as:

$$I(t) = I_0 \left(e^{-\alpha t} - e^{-\beta t} \right) \quad (2)$$

where I_0 is the amplitude, α the attenuation constant of ion current, and β the attenuation constant of electron current. Since in general the velocity of electrons is much higher than that of ions, the value of β is much bigger than that of α . The equation can explain the mechanism of corona discharge to some extent, and it is widely accepted.

The Gaussian function can also achieve the approximation of electrical discharge current waveforms. The corona current described by the Gaussian function is written as:

$$I(t) = I_0 e^{-(t-b)^2/2\sigma^2} \quad (3)$$

I_0 is the peak amplitude, b the time that the peak value appears, and σ the kurtosis of wave crest. To ascertain the accuracy approximation of the measured current, Reid et al. [14] and Zhou et al. [15] have developed the conventional Gaussian function and indicate that the PD currents can be represented by the multiple-order Gaussian function [14, 15]. The current described by a multiple-order Gaussian function is shown as:

$$I(t) = \sum_k I_k e^{-(t-b_k)^2/2\sigma_k^2} \quad (4)$$

2.2. Principle of the BPNN Method and the New Model

Although the discussed four equations in Section 2.1 are widely accepted by researchers in application of investigating discharge performances, they can obviously only represent a class of currents with specific shapes. The shapes of these currents always have one single pulse in their waveforms, and the trends of all the waveforms are flat. However, this is impossible under most measurement conditions because the discharge will be influenced by many factors such as temperature, humidity, air pressure [16], structure of the discharge system [17] and even the measurement system [18]. Under these conditions, the measured current waveforms will be in the shape of multiple pulses or a single pulse with damped oscillation rather than a regular single pulse. Therefore, none of all these developed functions can fit the measured discharge currents with arbitrary shapes under different conditions with sufficiently high accuracy.

Artificial neural network technique has been highly developed and widely applied in many fields, such as computer science, artificial intelligence, automatic control, and information processing. More

than 80% artificial neural networks take the structure of BPNN or its changing style. BPNN is widely applied in functions approximation. If the number of neurons in the hidden layer is sufficient, a BPNN with two layers can approximate to any functions or curves with an arbitrary accuracy degree that researcher expected when the transfer-function of the hidden layer is *logsig* function, and the transfer function of the output layer is *purelin* function [19, 20]. Given this advantage of the BPNN, the curve fitting method by BPNN will be investigated to try to acquire a better matching of the measured corona current waveforms than before.

Figure 1 shows details of the BPNN structure [20, 21]. The BPNN has a structure with two layers. One is the hidden layer, and the other is the output layer. Each net layer is mainly composed of a number of neurons and a transfer function. The hidden layer has N neurons, while this value is one for the output layer. The vector \mathbf{t} is the time sequence of the corona current as the input of the BPNN, and its elements is t .

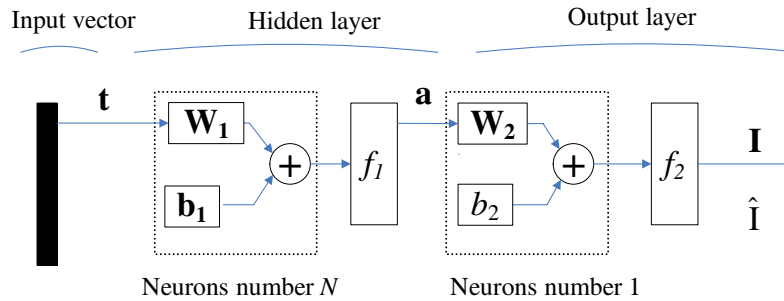


Figure 1. Structure of the BPNN.

\mathbf{I} is the magnitude vector of the corona current as the target output vector of the BPNN, and its element is the expected $i(t)$. $\hat{\mathbf{I}}$ is the output vector of the trained BPNN. It is the estimate of \mathbf{I} . \mathbf{W}_1 and \mathbf{W}_2 are the weight parameter vectors within the hidden layer and output layer, respectively. \mathbf{b}_1 is the threshold parameter vector within the hidden layer while b_2 is the threshold scalar in the output layer. Each neuron unit has an output value within one layer, and all the neurons' outputs consist of the output value of this layer. The layer's output, after experiencing some change, will be as the input of the next connected layer. The implement of the changing, which is a kind of mathematic mapping relationship, is dependent on the transfer function between layers. There are two common transfer functions f_1 and f_2 in BPNN shown in Fig. 1. f_1 stands for the transfer function *logsig*, and f_2 is the transfer function *purelin*. The transfer functions '*logsig*' and '*purelin*' are defined in the software MATrix LABoratory (MATLAB) widely accepted by the artificial neural network researchers, and they are described as follow

$$f_1(z) = \text{logsig}(z) = 1/(1 + e^{-z}) \quad (5)$$

$$f_2(z) = \text{purelin}(z) = z \quad (6)$$

where z is just a variable symbol. Function *logsig* is a logarithmic and nonlinear transfer function, and its output value is in $[0, 1]$ and often is used within the hidden layer. Function *purelin*, which is setup in the output layer, is a linear transfer function and only transfers the information without any change.

Firstly, an initial BPNN will be established by setting the number of neurons N within the hidden layer. Secondly, the established network is trained by the vectors \mathbf{t} and \mathbf{I} . Finally, we can gain the evaluation of \mathbf{I} , i.e., $\hat{\mathbf{I}}$ via extracting the parameters of the trained BPNN. From the calculation algorithms of the BPNN, the mathematic relation between $\hat{i}(t)$ and t can be derived as follow

$$\hat{\mathbf{I}} = f_2(\mathbf{W}_2 \mathbf{a} + b_2), \quad (7)$$

$$\mathbf{a} = f_1(\mathbf{W}_1 \mathbf{t} + \mathbf{b}_1), \quad (8)$$

$$\hat{i}(t) = b_2 + \sum_{j=1}^N w_{2j} \cdot \frac{1}{1 + e^{-(w_{1j} * t + b_{1j})}}, \quad (9)$$

where w_{1j} , b_{1j} and w_{2j} are the elements of the vectors \mathbf{W}_1 , \mathbf{b}_1 and \mathbf{W}_2 , respectively [19]. These vectors are four variables in an expression. The derivation is a general process which is not dependent upon curve shapes, and it is suitable for arbitrary current waveforms. If the number of neurons in hidden layer N is sufficient, the network is able to fit an arbitrary curve with any accuracy degree expected [18].

3. ANALYTICAL EXPRESSION FOR EXPERIMENTAL CORONA DISCHARGE CURRENT BASED ON BPNN METHOD

Three mathematic models, including the double exponential equation, multiple-order Gaussian equation and the new BPNN equation, will be applied to fit the corona currents, and also the comparisons of the match results among the three different models will be discussed. Considering the corona discharge easily influenced by many factors, the corona currents were measured from two different point-plane discharge systems. The differences, including the sizes and materials of the electrodes, gas gaps, applied voltages and ambient pressures, existed in between the two discharge systems. In system I with the copper electrodes, the applied voltage and pressure are 9.5 kV and 4×10^4 Pa for positive corona discharge and -2.0 kV and 1×10^3 Pa for negative corona discharge. In system II with the molybdenum electrodes, the applied voltage and pressure are 3.0 kV and 5×10^3 Pa for positive corona discharge and -1.53 kV and 1×10^4 Pa for negative corona discharge. The discharge system generates a corona current waveform that is more likely a single pulse while the current waveform from discharge system II composes of damped oscillation pulses.

3.1. Analytical Expressions for Simple Corona Currents

In the investigation of this paper, the corona currents measured from discharge system I were all nearly a single pulse in waveforms and treated as simple corona currents. Moreover, the positive current waveform has shorter duration and more oscillation in down time, while the negative current was polluted by environment noise in the measurement. All the current waveforms were fitted by using the double exponential function, Gaussian function and BPNN, respectively.

The waveform fitting results are shown in Fig. 2. Peak value is a significant character of the current waveform. Neither the waveform trend nor peak values are well fitted by the double exponential equation. The 2th order Gaussian function, which has the best fitting results within 10th order Gaussian function, has a better match than the double exponential equation, but it also does not match the peak values well. Both the double exponential function and Gaussian function cannot fit the current waveforms well. However, the BPNN with 20 neurons is in good agreement with current waveforms compared with the double exponential function and the 2th order Gaussian function. The neural network completely matches the current waveforms. Therefore, it is able to fit the details of the waveforms with a sufficiently high accuracy degree

The correlation coefficient r and MSE value of the two curves are usually treated as the quantification of curve fitting or function fitting effect. Here we mainly discuss the value MSE by reason of their relationship that the MSE will decrease as the r increases. The fitting MSE generated by three different functions is shown in Table 1. It indicates that the BPNN has the lowest MSE, of which the positive current can reach 10^{-4} ($r = 0.9988$), and the negative current is as low as 10^{-2} ($r = 0.9981$) in comparison with the other two functions. Since the negative corona current was mixed with environment noise, the fitting MSE value is higher than that of the positive current no matter what kind of functions used to fit the two current waveforms.

Table 1. The fitting MSE of the simple corona currents by using different equations.

MSE	double exponential equation	2th Gaussian equation	BPNN
positive current	0.0491	0.06539	5.4748e-4
negative current	23.2371	0.957	0.0438

All the former analysis about the fitting ability of different models was based on time domain; however, the evaluation parameters such as the goodness of fit and MSE are not able to absolutely explain all the fitting effects of different models. The reason is that these parameters just indicate a statistical error between the corona current and the fitting curve. This error cannot explain all the details about the fitting curve compared with the measurement current in frequency domain, and the spectrum analysis was rarely done. Sometimes researchers may pay more attention to the spectrum of corona current for better understanding its radiation field. Therefore, a frequency-domain analysis of the fitting results of different models is necessary.

The spectra of the corona currents and their different fitting curves are shown in Fig. 3. The x coordinate of the spectra figure stands for frequency component, and the unit is in MHz. The y coordinate is the value about fast Fourier transform (FFT) result of the current amplitude, and no unit is for it. The spectra of the currents indicate that the positive and negative corona currents have a similar

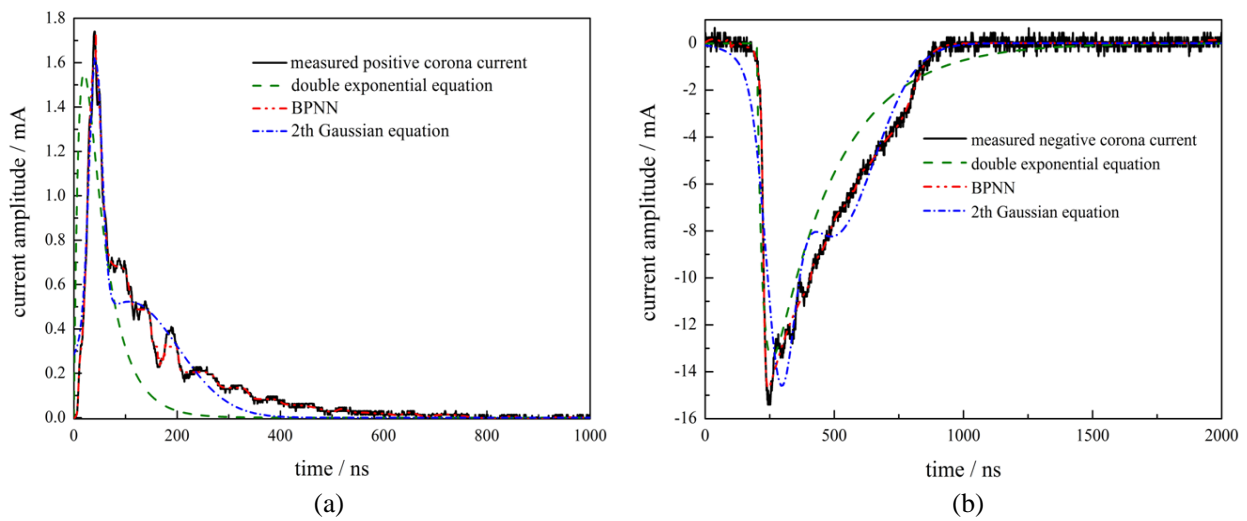


Figure 2. The fitting results of the measured simple corona currents in time domain: (a) positive corona, (b) negative corona.

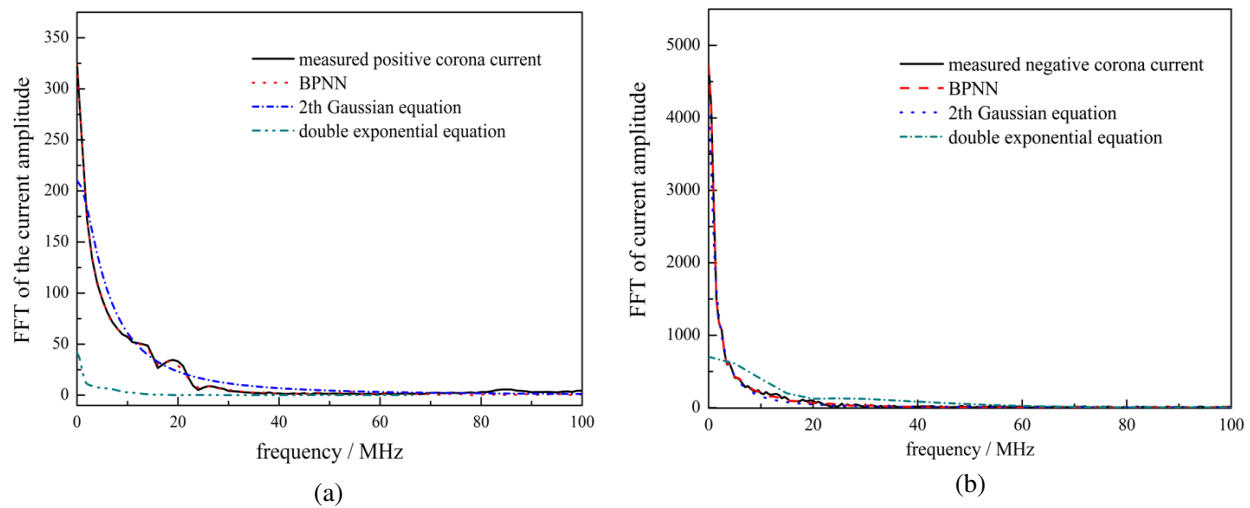


Figure 3. Spectra of the simple corona currents and the fitting curves: (a) positive corona, (b) negative corona.

spectrum distribution, and the upper frequency component is near 100 MHz. The spectra of the current curve fitting by the double exponential function, shown in Figs. 3(a) and (b), have great error compared with the measured corona currents. In comparison with the double exponential function, the 2th order Gaussian function behaves much better. When fitting the positive corona current, the spectrum of the curve matched by the Gaussian function shown in Fig. 3(a) generates a small mathematic error near the initial frequencies. Compared with the positive corona current, the spectrum of the negative current curve shown in Fig. 3(b) performs with great accuracy. However, the current curves shown in Figs. 3(a) and (b) matched by the BPNN, behave the best and have spectra mostly the same as the measured currents. Generally, no matter in time domain or frequency domain, the fitting curves by BPNN display great accuracy.

3.2. Analytical Expressions for the Complex Corona Currents

Corona discharge will be easily affected by the discharge environment, and the measured current displays complex waveforms which often show a damped oscillatory pulse instead of a single pulse in time domain at most of the time. Investigation [14] indicates that these complex currents can achieve a significantly better match by higher order Gaussian functions compared with the Wanninger function and double exponential function. Based on the investigation, the BPNN method proposed in this paper will be used to fit this kind of complex corona currents, and a comparison with the multiple-order Gaussian function will be discussed.

The corona currents measured from discharge system II are all a damped oscillatory pulse in waveforms and can be treated as complex corona currents. According to [14], the order of the Gaussian functions was selected within 10th, and the fitting results are shown in Fig. 4. As shown in Figs. 4(a) and (b), the Gaussian functions with the order ranging from 4th to 7th have better fitting results of positive corona current, while the better order to the negative corona current is from 6th to 8th. These fitting curves can follow the changing tendency of a series of peaks and troughs of the current waveforms, but they cannot offer accurate fitting value point to point, especially at the peak values of the currents. Moreover, the Gaussian function cannot establish a united analytical expression model for the currents even if they are measured from one discharge system, because the expressions have different orders. When fitting the positive corona current, the 6th order Gaussian function has the best behaviors, while to the negative corona current, the 8th order Gaussian function has the best fitting result. Compared with the Gaussian function, the fitting current curves by BPNN with 35 neurons, shown in Figs. 5(a) and (b), can almost fit the corona currents no matter positive or negative. According to the fitting error data shown in Table 2, the MSE value of the 6th order Gaussian function fitting positive corona current is 2.7605e-5 while this value is 2.1447e-6 ($r = 0.9824$) for BPNN. At the same time, the MSE of the 8th order Gaussian functions fitting negative corona current is 1.0068e-5 while this value is 3.5147e-6 ($r = 0.9491$) for BPNN. The fitting MSE by BPNN is obviously much lower than that of the Gaussian functions. Compared with multiple-order Gaussian function, the BPNN also performs much better.

A frequency domain analysis and comparison between the fitted currents and the measured corona currents are also necessary. The FFT results of the current amplitudes are shown in Figs. 6(a) and (b), respectively. The spectra of the measured currents indicate that the positive corona current spectrum has a narrower bandwidth than the negative corona current. The upper frequency component of the former is near 350 MHz while this value is near 500 MHz of the latter so their spectra distribution has much difference. According to the figure, we conclude that the spectra of Gaussian functions cannot fit the spectra of currents well neither the tendency nor the peak values. However, BPNN is able to achieve a significantly better match as can be seen.

Table 2. The fitting MSE of the complex corona currents by using different equations.

MSE	Gaussian equation	BPNN
positive corona current	(6th order) 2.7605e-005	($N = 35$) 2.1447e-06
negative corona current	(8th order) 1.0068e-005	($N = 35$) 3.5147e-06

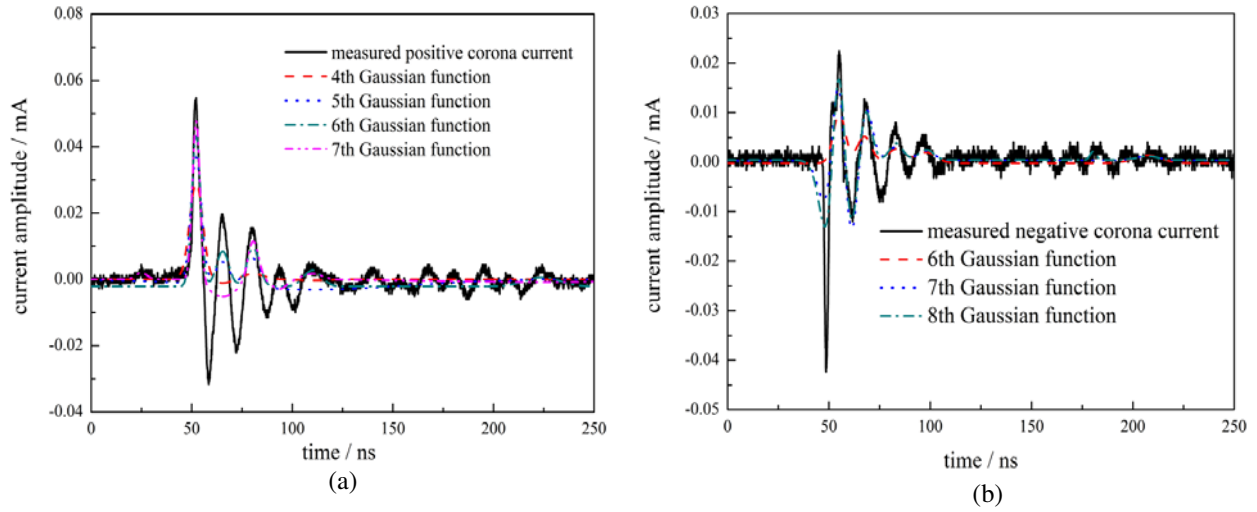


Figure 4. Fitting results of the measured complex corona currents by Gaussian functions in time domain: (a) positive corona, (b) negative corona.

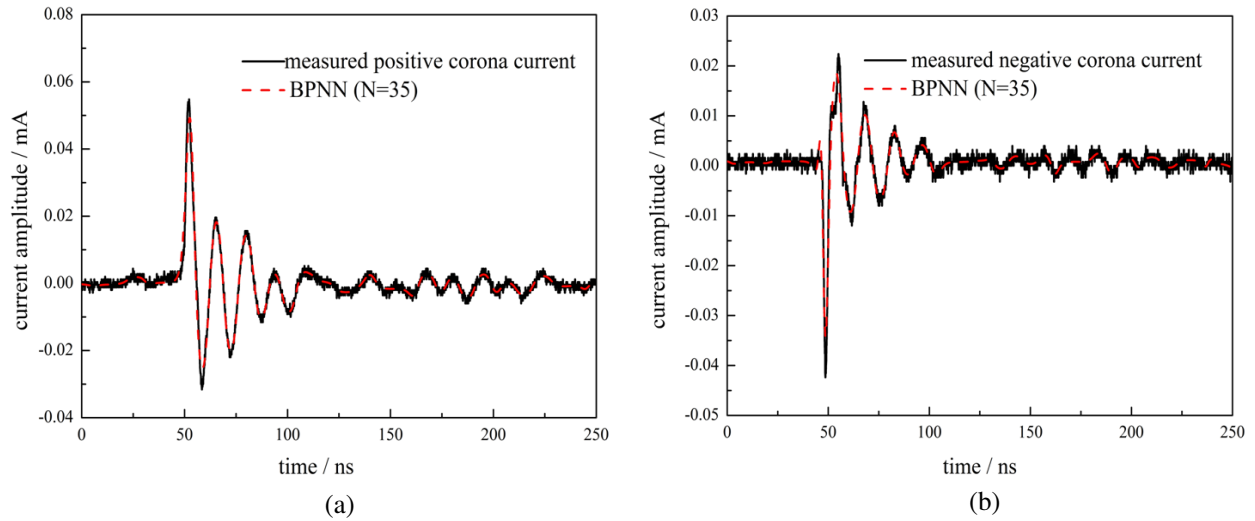


Figure 5. Fitting results of the complex corona currents by BPNN in time domain: (a) positive corona, (b) negative corona.

3.3. The Selection of the Neurons Number, i.e., N within BPNN Hidden Layer

In order to select an appropriate N value, a criterion is proposed. The criterion is mainly dependent on two parameters, i.e., the correlation coefficient r and MSE, especially parameter r because MSE is the absolute error determined by r . With r increasing, the MSE will decrease. The coefficient r will be calculated by comparing the BPNN output current and the measured current. We can set up a threshold value r_0 , of which the value is always less than 1 but needs sufficiently close to 1. Once r is larger than r_0 , the corresponding N can be treated as an appropriate one. This is a self-adaptive selecting processed by computer.

When using the BPNN method to fit one current waveform, the number of neurons, N , has many choices. For example, when fitting the simple and complex corona currents, N are selected as 20 and 35, respectively, but they are not the only choice. The details of the MSE value changing with the value N are shown in Fig. 7. With N increasing, the network matches the current shapes better and achieves a lower MSE. Generally, the best choice of N always depends on not only current waveforms, but also engineering requirement, for the researchers are interested in the better match but with a simpler

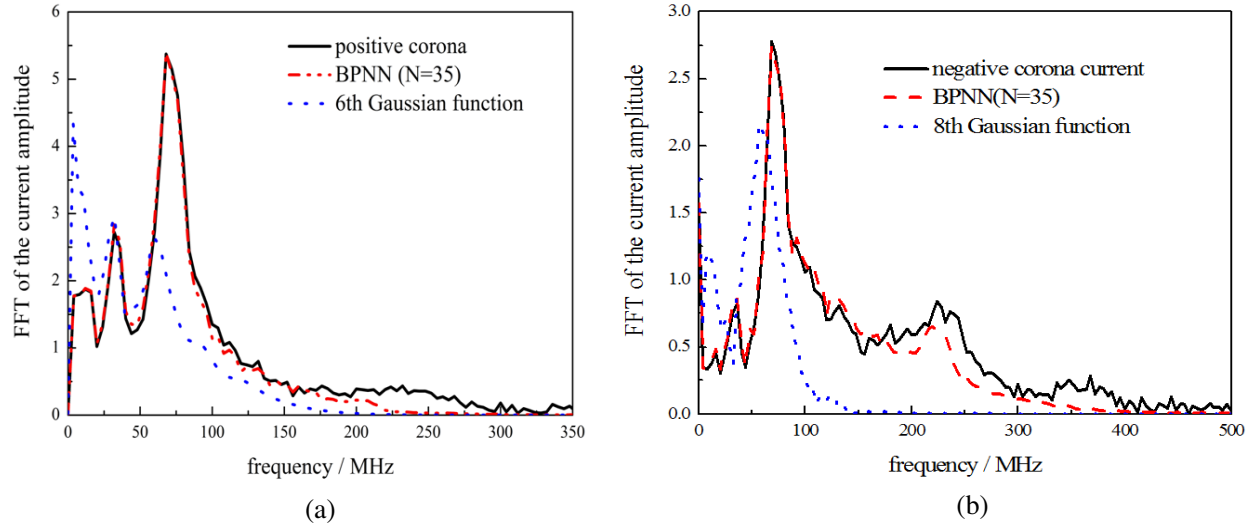


Figure 6. Spectra of the complex corona currents and the fitting curves: (a) positive corona, (b) negative corona.

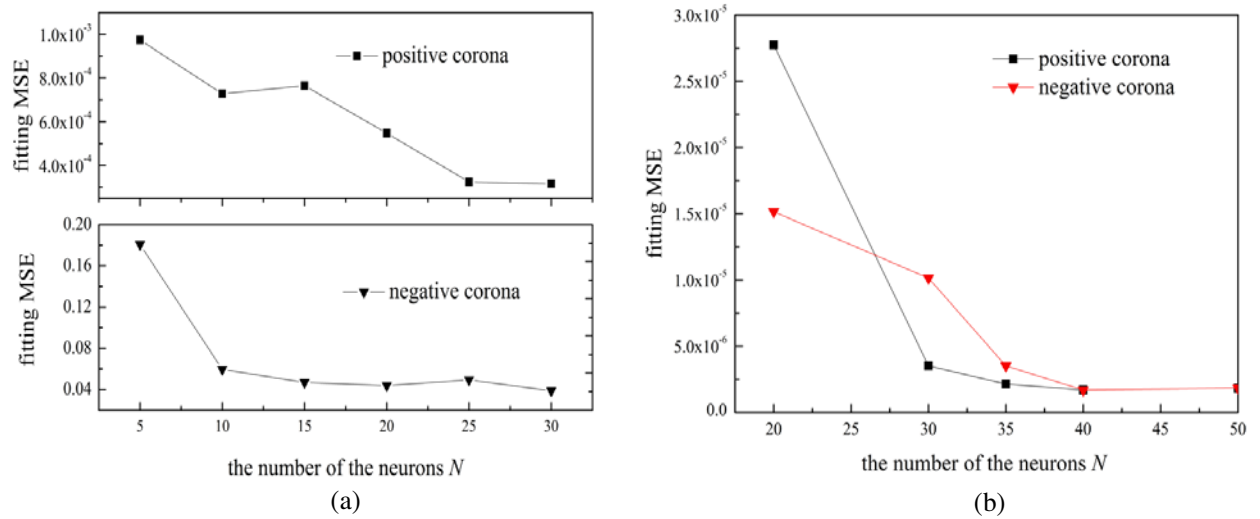


Figure 7. The fitting MSE of corona currents by using BPNN: (a) the simple corona current, (b) the complex corona current.

configuration of the current expression. In this paper, because of the extremely low MSE and it will not decrease quickly when the N exceeds some value, 10 to 20 neurons are enough for the simple corona currents and 35 to 50 for the complex corona currents. Considering the complexity of the analytical expressions, N was selected as 20 for the simple corona currents ($r = 0.9988$ for positive corona and 0.9981 for negative corona) and 35 for the complex corona currents ($r = 0.9824$ for positive corona and 0.9491 for negative corona). It is obvious that N will increase as the current waveform becomes complex.

3.4. The Analytical Expressions for the Corona Currents Fitted by BPNN

By extracting the parameters of the trained BPNN, the analytic expressions for currents can be described as formula (9). There are four parameters in an expression, i.e., \mathbf{W}_1 , \mathbf{b}_1 , \mathbf{W}_2 and \mathbf{b}_2 . For example, the parameters of the simple negative corona current are described as follows when N is 20, and they are shown in Table 3.

Table 3. Parameters extracting from BPNN with $N = 20$ for the simple negative corona current.

Parameters	\mathbf{W}_1	\mathbf{b}_1	\mathbf{W}_2^T	b_2
	-0.0444	29.3819	-1.3309	
	-0.0155	106.1073	-1.5025	
	-0.0347	100.2075	-0.3872	
	1.3449	-131.4275	-0.4822	
	0.1171	88.4273	0.1577	
	-0.0184	-82.5263	0.1221	
	0.1737	-99.4081	-2.9147	
	-0.0593	28.6477	-1.5202	
	0.0005	-64.8419	0.0279	
value	-0.2787	114.2099	-0.6972	-2.7771
	-0.0072	52.9408	-3.6366	
	0.0108	-1.9714	18.3945	
	0.1201	-68.8183	4.1105	
	0.1175	-225.7983	0.1303	
	0.0292	-23.5482	4.0303	
	0.0052	24.6062	-4.3654	
	0.1173	-23.5056	-2.6408	
	-0.2256	50.6742	14.2710	
	0.0408	-4.2377	50.6112	
	0.0372	-3.9144	-58.5929	

The analytic expression for the current is as follow

$$\hat{i}(t) = -2.7771 + \left[-1.3309 \cdot \frac{1}{1 + e^{-(0.0444t + 29.3819)}} + (-1.5025) \cdot \frac{1}{1 + e^{-(0.0155t + 106.1073)}} \right. \\ \left. + \dots + 50.6112 \cdot \frac{1}{1 + e^{-(0.0408t - 4.2377)}} + (-58.5929) \cdot \frac{1}{1 + e^{-(0.0372t - 3.9144)}} \right]. \quad (10)$$

The parameters of the complex negative corona current fitted by BPNN with 35 neurons are shown in Table 4.

The analytic expression for the current is as follow

$$\hat{i}(t) = -98.3811 + \left[(-0.0009) \cdot \frac{1}{1 + e^{-(7.84 \cdot 10^8 t - 194.6712)}} + (-24.4939) \cdot \frac{1}{1 + e^{-(7.84 \cdot 10^8 t - 186.533)}} \right. \\ \left. + \dots + 0.1451 \cdot \frac{1}{1 + e^{-(7.84 \cdot 10^8 t - 2.2993)}} + (-0.1455) \cdot \frac{1}{1 + e^{-(7.84 \cdot 10^8 t - 37.0874)}} \right]. \quad (11)$$

3.5. The Characters of the BPNN Model Comparing with Other Function Models

Firstly, a mathematic function that can be treated as an analytical model for the current expression must be uniform in structure. Against different currents, the analytical expressions extracted from the BPNN have the same structure which is suitable for corona currents of arbitrary shapes, and there are total four parameters. Secondly, according to formulas (9)–(11), we know that the element number of the total parameters within the analytical expression for a corona current fitted by BPNN is $3 \times N + 1$. If the order value is also N when selecting the multiple-order Gaussian equation shown in formula (4) to fit the corona currents, then there are three parameters, and their element number is $3 \times N$. At the same time, this value is only 3 for the double exponential equation as shown in formula (2). Compared

Table 4. Parameters extracting from BPNN with $N = 35$ for the complex negative corona current.

Parameters	$\mathbf{W}_1(*7.84\text{e}8)$	\mathbf{b}_1	\mathbf{W}_2^T	b_2
	1	-194.6712	-0.0009	
	1	-186.533	-24.4939	
	-1	186.5131	-49.0861	
	1	-186.4932	-24.5930	
	1	-174.3207	0.0017	
	-1	168.4030	0.0024	
	1	-159.5896	0.0609	
	-1	159.4466	0.0611	
	1	-151.1076	0.0045	
	-1	146.9140	0.0056	
	-1	142.0963	-0.0023	
	-1	127.0198	-0.5716	
	-1	126.9972	0.5735	
	-1	121.1478	-0.0025	
	1	-114.3777	-0.0020	
	1	-109.0582	0.0031	
	1	-102.6365	-38.4937	
value	-1	102.6364	-38.4918	-98.3811
	1	-94.0846	0.0003	
	1	-82.8406	0.0036	
	1	-78.6056	-0.0077	
	-1	72.5242	-0.0077	
	-1	66.8941	0.0123	
	1	-62.3585	0.0177	
	1	-56.0786	-0.0211	
	-1	50.6104	-0.0250	
	-1	44.5791	0.0369	
	1	-37.0847	67.4762	
	-1	36.9547	155.9594	
	1	-36.7733	143.3977	
	-1	36.6410	54.8906	
	-1	14.9892	-24.9728	
	1	-14.9892	-24.9726	
	1	-2.2993	0.1454	
	1	-2.2868	-0.1455	

with double exponential equation or multiple-order Gaussian equation, the total element number of the parameters within the BPNN model is larger. However, the BPNN indeed displays its great advantage of an extremely accurate approximation of the arbitrary current waveform especially for the complex corona currents, and this is what most of engineers are hoping for. Obviously, it is impossible for the multiple-order Gaussian equation, even increasing its order N the same as BPNN. On the other hand, the BPNN trains data quite fast by computer usually spending 2 to 10 seconds, and therefore, the complexity of the current expression parameters can be ignored compared with the model's great advantage. Further investigation will focus on developing the definition of each parameter in the model which is not explained here.

4. CONCLUSIONS

In order to establish a unified mathematic model for corona currents, a novel curve fitting method based on BPNN technique is applied to describe the analytical expressions for measured corona currents. The neural network has two layers including the hidden layer and output layer, and it is trained by the measured corona current data. The analytical expression for an arbitrary current can be gained via extracting the weights and thresholds parameters of the trained network. The real corona currents were measured from two point-plane electrode discharge systems. Considering the waveforms, the corona currents from system I are simple, while the currents from system II are complex. Different models, including the double exponential equation, multiple-order Gaussian equation and BPNN, were used to fit the corona currents, and the results were analyzed in time domain and frequency domain. The fitting result of the currents with simple waveforms indicates that the Gaussian equation performs much better than the double exponential equation, but both of the equations can fit neither the waveforms nor the spectra of the complex currents. However, by using trained BPNN, we can get the fitting curves for both waveforms and spectra the same as the measured corona currents no matter simple or complex. The fitting error, i.e., MSE level, can be as low as 10^{-6} .

ACKNOWLEDGMENT

This work was supported by the National Natural Science Foundation of China (61172035 and 51277181). The authors would like to thank Qimeng Wu for discussion.

REFERENCES

1. Liu, X. H., W. He, F. Yang, H. Y. Wang, R. J. Liao, and H. G. Xiao, "Numerical simulation and experimental validation of a direct current air corona discharge under atmospheric pressure," *Chin. Phys. B*, Vol. 21, No. 7, 0752011-10, 2012.
2. Morrow, R., "Theory of positive corona in SF₆ due to a voltage impulse," *IEEE Trans. Plasma Sci.*, Vol. 19, No. 2, 86–94, 1991.
3. Morrow, R., "Theory of electrical corona in SF₆," *Nucl. Instrum. Methods Phys. Res. A*, Vol. 382, 57–65, 1996.
4. Morrow, R., "The theory of positive glow corona," *J. Phys. D: Appl. Phys.*, Vol. 30, 3099–114, 1997.
5. Wangninger, G., "Discharge currents of free moving particles in GIS," *10th Int.Symp.on High Voltage Engineering Dielectrics and Insulation*, Vol. 2, 219–222, Montreal, QC, Canada, 1997.
6. Arin, N. and W. Blumer, "Transient electromagnetic fields due to switching operations in electric power systems," *IEEE Trans. Electromagn. Compat.*, Vol. 29, No. 3, 233–237, 1987.
7. Judd, M. D., O. Farish, and B. F. Hampton, "Modelling partial discharge excitation of UHF signals in waveguide structures using Green's functions," *IEE Proc. Meas. and Technol.*, Vol. 143, No. 1, 63–70, 1996.
8. Maruvada, P. S., *Corona Performance of High-Voltage Transmission Lines*, 114, Research Studies Press LTD, Baldock, 2000.
9. Judd, M. D., "Using finite difference time domain techniques to model electrical discharge phenomena," *IEEE Conf. on Electrical Insulation and Dielectric Phenomena*, 518–521, Victoria, BC, Canada, 2000.
10. Nayak, S. K. and M. J. Thomas, "An integro-differential equation technique for the computation of radiated EMI due to corona on HV power transmission lines," *IEEE T Power Delivery.*, Vol. 20, No. 1, 489–493, 2005.
11. Nayak, S. K. and M. J. Thomas, "A novel technique for the computation of radiated EMI due to corona on HV transmission lines," *IEEE International Symposium on Electromagnetic Compatibility*, 738–742, August 18–22, 2003.

12. Fu, H. Z., Y. J. Xie, and J. Zhang, "Analysis of corona discharge interference on antennas on composite airplanes," *IEEE Trans. Electromagn. Compat.*, Vol. 50, No. 4, 822–827, 2008.
13. Liao, R. J., F. F. Wu, X. H. Liu, F. Yang, L. J. Yang, Z. Zhou, and L. Zhou, "Numerical simulation of transient space charge distribution of DC positive corona discharge under atmospheric pressure air," *Acta Phys. Sin.*, Vol. 61, No. 24, 245201-11, 2012.
14. Reid, A. J., M. D. Judd, B. G. Stewart, and R. A. Fouracre, "Partial discharge current pulses in SF₆ and the effect of superposition of their radiometric measurement," *J. Phys. D: Appl. Phys.*, Vol. 39, 4167–4177, 2006.
15. Zhou, Q., J. Tang, M. Tang, Y. B. Xie, and M. J. Liu, "Mathematic model of four typical defects for UHF partial discharge in GIS," *Proceedings of the CSEE*, Vol. 26, No. 8, 99–105, 2006.
16. Merbahi, N., M. Yousfi, and J. P. Gardou, "Electric and spectroscopic analysis of surface corona discharges in ambient air and comparison with volume corona discharges," *IEEE Trans. Plasma Sci.*, Vol. 40, No. 4, 1167–1176, 2012.
17. Daisuke, O., "Time-lag properties of corona streamer discharges between impulses sphere and dc needle electrodes under atmospheric air conditions," *Rev. Sci. Instrum.*, Vol. 84, 024702, 2013.
18. Wang, P., G. X. Zhang, J. Zhou, and C. Gu, "Optical micro-current transducer for the measurement of corona discharge current under high voltage environment," *Instrumentation and Measurement Technology Conference*, 1–3, Warsaw, Poland, May 1–3, 2007.
19. Hornik, K., "Multilayer feedforward networks are universal approximators," *Neural Networks*, Vol. 2, 359–366, 1989.
20. Wu, Q. M., M. Wei, G. H. Fan, and J. Liu, "Analytical expressions of electrostatic discharge current based on the BP neural network," *High Voltage Engineering*, Vol. 38, No. 11, 2912–2918, 2012.
21. Wu, Q. M. and M. Wei, "A mathematical expression for air ESD current waveform using BP neural network," *Journal of Electrostatic*, Vol. 71, 125–129, 2013.